Manuscript Details

Title: Multiple-fault Detection and Identification Scheme based on Hierarchical Self-Organizing Maps applied to an Electric Machine

Author names and affiliations: Juan Jose Saucedo-Dorantes[a], Miguel Delgado-Prieto[b], Rene de Jesus Romero-Troncoso[a] and Roque Alfredo Osornio-Rios[a].

[a]HSPdigital CA-Mecatronica, Engineering Faculty, Autonomous University of Queretaro, San Juan del Rio 76806, Mexico.

[b]MCIA Research Center, Department of Electronic Engineering, Technical University of Catalonia (UPC), Spain.

Corresponding author. Miguel Delgado-Prieto[b]; miguel.delgado@mcia.upc.edu

Multiple-fault Detection and Identification Scheme based on Hierarchical Self-Organizing Maps applied to an Electric Machine

***Abstract*— Strategies of condition monitoring applied to electric motors play an important role in the competitiveness of multiple industrial sectors. However, the risk of faults coexistence in an electric motor and the overlapping of their effects in the considered physical magnitudes represent, currently, a critical limitation to provide reliable diagnosis outcomes. In this regard, additional investigation efforts are required towards high-dimensional data fusion schemes, particularly over the features calculation and features reduction, which represent two decisive stages in such data-driven approaches. In this study, a novel multiple-fault detection and identification methodology supported by a feature-level fusion strategy and a Self-Organizing Maps (SOM) hierarchical structure is proposed. The condition diagnosis as well as the corresponding estimated probability are obtained. Moreover, the proposed method allows the visualization of the results while preserving the underlying physical phenomenon of the system under monitoring. The proposed scheme is performed sequentially; first, a set of statistical-time based features is estimated from different physical magnitudes. Second, a hybrid feature reduction method is proposed, composed by an initial soft feature reduction, based on sequential floating forward selection to remove the less informative features, and followed by a hierarchical SOM structure which reveals directly the diagnosis and probability assessment. The effectiveness of the proposed detection and identification scheme is validated with a complete set of experimental data including healthy and five faulty conditions. The accuracy's results are compared with classical condition monitoring approaches in order to validate the competency of the proposed method.**

***Keywords*— condition monitoring; fault diagnosis; feature estimation; feature reduction; induction motor; self-organizing feature maps; time series analysis; sequential selection; stator currents; temperatures; vibrations.**

1 INTRODUCTION

Fault detection and identification have become critical aspects to allow a timely and accurate application of maintenance strategies to the modern industry machinery [1]-[3]. Most of the industrial applications are supported by electric motor which are used in the transformation of electrical energy into mechanical energy, in this regard, Induction Motors (IM) have been represented the most extended technology of rotating electrical machine due to its reliability, low cost and robustness [4]. However, despite of its characteristics, the appearance of unexpected faults may occur during its useful life period, thus, affecting the machinery availability, the industrial productivity and the economic benefits of the related industrial process. In this regard, condition monitoring strategies applied to the fault detection and identification are playing an important role to increase and ensure the availability of most of the industrial machinery.

The malfunctioning problems that can occur in IM are, mainly, due to the appearance of electrical and mechanical faults [5]-[7]. In this sense, the most common electrical faults are those associated with problems in the stator and rotor windings, such as broken rotor bars and short-circuits; while mechanical faults are those related to problems of eccentricity and misalignment that are generated due to damages in bearings and couplings [8]-[10]. Currently, in most of the industrial processes, different variables are easily available, such as temperatures, stator currents, voltages, even mechanical vibrations [11]-[13]; indeed, the non-invasive installation of sensors is one of the most preferred strategies to assess the condition in industrial processes [11]. In this regard, a great deal of data-driven diagnosis methods have been proposed to identify the appearance of faults in IM-based electromechanical systems, yet, although advantageous results have been obtained, most of these proposals have been focused to address single fault modes [14]-[15]. Thereby, signal processing approaches that use a unique physical magnitude, usually stator currents or vibrations, represent the most common strategy for condition monitoring of electric machines [9], [16]. Nevertheless, the detection and identification capabilities of current condition monitoring approaches applied to electric motor faults must overcome new challenges. Specifically, multiple and non-expected causes of faults must be detected and recognized during the regular operation of electric motor based machinery. Indeed, this assumption represents a serious issue to allow a practical implementation of condition monitoring strategies in industrial systems,

since the effects of different faults can be hidden or overlapped during the inspection.

Condition monitoring strategies based on the combination of different physical magnitudes represent the most coherent approach aiming to provide the machine condition [12], [17]. In this regard, time domain, frequency domain and time-frequency domain are the three well-known approaches that have been widely applied during the characterization of the available physical magnitudes [2], [18]. However, although classic techniques based on frequency and time-frequency domain have been widely applied, most of these techniques requires a deep knowledge of the fault effects over the resulting frequency distributions of the physical magnitudes [19]-[22]. Moreover, as background noise and other unconcerned components may mask the patterns, some signal enhancement techniques are required to preprocess the original signals. Thus, considering an electromechanical system, where different components take place, it is possible that similar failure effects may be induced by different causes. For example, in industrial processes where rotating machinery is involved, the appearance of malfunctioning conditions, such as unbalance and misalignment, produce similar components in the vibrational spectrum at the rotating frequency and its corresponding harmonics [20]. Thereby, due to specific faults may appear hidden or overlapped, the fault identification represents a major issue when multiple fault sources are simultaneously considered.

Although the consideration of a high-dimensional set of numerical features could increases the fault identification capability during the electric machine condition assessment, the inevitably calculation of redundant and non-significant information may affect the posterior fault detection and identification performance. In this regard, aiming to avoid low fault diagnosis performances and overfitted results, dimensionality reduction procedures are recommended to be applied in condition monitoring strategies [23]. The most well-known classical dimensionality reduction techniques that have been widely applied are Principal Component Analysis (PCA), and Linear Discriminant Analysis (LDA) [24]-[25]. Nevertheless, these two dimensionality reduction approaches are based on a specific objective function; thereby, PCA deals with the data variance maximization, while LDA aims to maximize distances between different data sets [26]-[27]. Such differences in criteria allow the combination of dimensionality reduction approaches with classification algorithms aiming to achieve specific classification ratios [28]. Indeed, this strategy, also known as wrapper approach, uses a predefined induction algorithm and its resulting performance as evaluation criteria during the dimensionality reduction process. This method implies higher computational costs, but, since the feature subsets resulting from a wrapper approach are evaluated by the modelling accuracies, significance of the reduced feature set is generally increased. In this regard, one of the most common wrapper-based methods is supported on the use of Sequential Floating Feature Selection (SFFS) [24], [29].

Finally, the classification algorithms play an important role in such data-driven condition monitoring methodologies performing the automatic detection and identification of the electric motor condition. In this regard, Neural Networks (NN), and fuzzy inferred systems represent the most commonly used classical classifiers [2], [30]-[31]; besides, classifiers like *k*-nearest neighbors, decision trees, Bayesian networks and support vector machines, have been also used [15], [17]. However, due to these techniques follow a supervised training approach, their application is usually related with the enhancement of the classification ratios. In this sense, according to Shannon's rate-distortion theory, mutual dependencies among various sources and between the input and output spaces contain the actual intrinsic dimension of the data, and allows avoiding over-fitting responses of the classification algorithms. Thereby, the application of unsupervised learning approaches represents the most coherent processing procedure to retain the underlying physical phenomenon of the system under monitoring reducing overfitting risks. Regarding this problem, manifold learning methods have been implemented with the aim of preserving the information in a lower dimensional space [32]-[33]. Thus, Self-Organizing Maps (SOM), are among the most used approaches. The SOM are based on a neural network grid that preserves most of the original distances between feature vectors representations in the original feature space; moreover, it also allows the mapping of high-dimensional input data onto a 2-dimensional space [34]. Although SOM leads to model the original data distribution following an unsupervised approach, each of the

neuron units used during the original space characterization can be associated with a class label, from which a diagnosis inference can be carried out during the assessment of new measurements.

Considering such state of the art in regard with the current challenges on condition monitoring applied to electrical machinery, the main contribution of this research work lies on the proposal of a novel detection and identification scheme. The proposed methodology is based on a feature-level fusion approach where the pattern characterization capabilities of different physical magnitudes are enhanced in order to deal with multiple fault scenarios, thus, reducing the false negative detection ratios and improving the faults identification. The contributions include also the validation of a hierarchical SOM structure as powerful pattern characterization tool with data visualization capabilities. The novelty of the proposed fault detection and identification scheme include the consideration of a statistical-time based feature reduction stage by means of a soft dimensionality reduction, and a hierarchical classification structure supported by SOM for data modelling and fault diagnosis. In order to validate the competency of the proposed diagnosis methodology, a complete set of experimental data is acquired during the working condition of an electromechanical system, where five different conditions are experimentally evaluated. Also, the results are compared with a classical fault detection and identification approach based on PCA and LDA for feature reduction and NN for classification. Notice that this is the first time that this data fusion based hierarchical diagnosis scheme is applied, and the obtaining results are promising to be suitable for multiple condition monitoring applications.

2 THEORETICAL BACKGROUND

2.1 Data-driven condition monitoring

Most of the classic condition monitoring strategies are based on pattern recognition approaches and their structures are related with the accomplishment of three main tasks as follows. First, the calculation of numerical sets of features from the available physical magnitudes through the application of classic techniques based on the analysis in the time domain, frequency domain and time-frequency domain. Second, the consideration of feature reduction stages for highlighting the hidden fault characteristic patterns and for compressing the available information computed during the feature calculation. Finally, third, in a classification stage, the identification of the pattern among different classes, the fault conditions, is performed.

In this regard, classifications algorithms that are directly fed by raw data sets of numerical features are susceptible to decrease the performances of their outcomes; aiming to overcome this issue, feature reduction processes have been normally applied by means of linear techniques to enhance specific characteristics; such as the data variance maximization through PCA, or improve the separation among different classes (operating conditions) by means of LDA. However, the limitations of such classic feature reduction approaches that have been pointed out by several studies indicate that problems usually are presented for dealing with large and disconnected data sets, and this is due to classic structures seek for global structures of the available data [35]-[36]. Moreover, a feature vector is composed by a set of D calculated features from the available physical magnitudes, and the obtained feature vectors are represented into an D-dimensional space. Indeed, the information included in such D-dimensional space mostly has nonlinear structures; thereby, in order to overcome such drawbacks, manifold learning methods, as SOM, are being developed as superior approaches in the last years [37]-[38].

2.2 Self-organizing maps

The SOM is an unsupervised learning algorithm based on neural networks, and its main objective is the preservation of the topological properties of a D-dimensional input data space during its projection to a reduced d-dimensional output space. As a result of its application, a predefined 2-dimensional output space represented by a neural network grid is obtained; indeed, the use of hexagonal or rectangular grids is the most preferred neural structures for representation [38]. The SOM neural network is composed by a set neurons which are spatially distributed and interconnected among them; where, each neuron of the grid represents a Matching Unit (MU). In this regard, the mapping is carried out by means of allocating each input data vector, din_j, $j=1...M$, to

one of the considered neurons. Indeed, those closest weight vectors are called the Best Matching Unit (BMU). Thus, the position vector for each input data in the output space, $dout_j$, is defined by the position that the corresponding BMU takes in the grid. During the training procedure of the SOM grid, the minimization of a cost function based on the error estimation is the goal to achieve.

Classically, the performance of a trained SOM grid is evaluated though the estimation of the average quantization error, *Eq*. The *Eq* represents the average distance from each input data vector to its corresponding BMU, that is, the so called local topology mean error is estimated by following (1).

$$E_q = \frac{\sum_M^{j=1} \| din_j - dout_j \|}{M} \tag{1}$$

From a practical point of view, before to the training of the SOM network, the neuron grid composed by a predefined number of matching units is randomly initialized within the input data space, Fig. 1(a). Then, during the training, Fig. 1 (b), the MU's grid is successively adapting the weights wn_i aiming to retain as much as possible the local topology of the measurements characterized in the initial feature space. Finally, in the trained grid may be evaluated new data, Fig. 1 (c), and through its evaluation, the Euclidean distance of a new measurement to each MU is computed. Thus, the nearest MU which is considered the BMU is then activated. As a result of this procedure, the input data space can be modelled by a small number of MU. Yet, although SOM is an unsupervised learning approach, during the training process, each MU can be associated to a specific machine condition through a supervised labelling process. Thereby, later, for a new measurement assessment, its diagnosis outcome can be obtained. It must be noted that, in the proposed fault detection and identification scheme, the quantization error, classically used only as a cost function during the training process, takes an important significance. Thus, during the assessment of a new measurement, its novelty degree in regard with the reference data distribution can be quantified. Hence, a high or low reliability of the diagnosis outcome will result from a high or low quantization error, respectively.

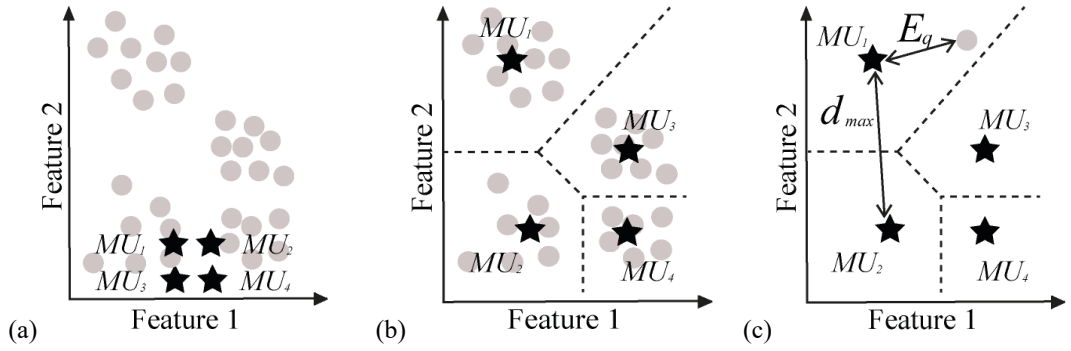

Fig. 1. Representation of the self-organizing mapping procedure in a 2-dimensional input and output spaces. (a) Input data samples, ●, and a randomly initialized 2 x 2 neuron grid, ★. (b) Resulting training process. The dotted lines represent the memberships regions of the matching units considering Euclidian distances. The maximum distance between MU, d_{max}, corresponds to MU_1 and MU_2. (c) Assessment of a new input data sample, ●. Assignation to MU_1 as closest matching unit with the corresponding individual quantization error E_q.

3 PROPOSED MULTI-FAULT DETECTION AND IDENTIFICATION METHODOLOGY

The proposed diagnosis methodology for the detection and identification of multiple faults in an electrical motor based actuator consists of four stages as Fig. 2 depicts. First, a set of available physical magnitudes are acquired in a data acquisition stage; preferably, the acquired information should include the occurrence of vibrations in the radial and tangential plane of the kinematic chain, one to three stator current phases, and some temperature signals distributed over the electric motor, for instance, three of them placed near the drive-end-

bearing, the non-drive-end bearing, and the motor chassis. Second, in order to build a consecutive set of samples, the acquired signals are segmented in equal part of one second and then characterized by performing a feature calculation, in this regard, a set of ten statistical time-based features is computed from each segmented part of the available signals. The proposed set of features considers: mean ($\bar{x}$), RMS, standard deviation (σ), variance (σ^2), shape factor (SF_{RMS}), crest factor (CF), latitude factor (LF), impulse factor (IF), skewness (S_k) and kurtosis (Ku); indeed, these features have been successfully used in other works in which its mathematical equations may be found [18]. Consequently, 20 statistical time features are estimated from the two vibration signals, 10 statistical time features from one motor stator current, and 30 statistical time features from the three temperature signals; therefore, each measurement over the electric motor is characterized by a resulting data set of consecutive samples composed by 60 statistical time-based features. Next, third, aiming to increase the characterization capabilities, the feature reduction is proposed to be replicated in terms of three specific condition groups to be evaluated, that is: (i) healthy against the rest of faulty conditions, (ii) among all faulty conditions and, finally, (iii) among severity degrees of each fault if available. This organization of the data allows to improve the filtering and retaining of those features with the best discriminative capabilities and that better characterize each one of the conditions, this filtering is proposed to be carried out by a soft dimensional reduction approach based on feature selection through SFFS. Fourth, following the same condition groups, the mapping of the data distributions to perform the posterior diagnosis is carried out by means of the proposed hierarchical structure based on SOM.

In this regard, during the on-line assessment of the proposed methodology over a new measurement, the feature selection as well as diagnosis stages are executed iteratively. The application of a hierarchical structure as a diagnosis scheme allows to address the assessment of multiple faults from a general point of view towards the particular. Thus, in a first layer, a two-class problem is considered with the aim of distinguish between the healthy condition and the rest of faulty conditions (generalized as faulty condition), that is, to determine *whether a fault condition is present or not*. In case of a healthy condition diagnosis, the corresponding probability degree is provided, and the diagnosis procedure ends. Otherwise, the next diagnosis layer is evaluated in regard with the identification of the fault among the considered machine faulty conditions. Once identified, the corresponding probability fault degree is also provided. Thus, in this second layer *which fault is taking place* is determined. Finally, in case of severity degrees availability for some of the diagnosed faults, a third diagnosis layer follows, from which the corresponding probability degree is estimated also, that is, to determine the *fault severity degree*. In this sense, from a general perspective, the condition assessment of the electromechanical system is addressed in cascade, as the flowchart of Fig. 3 depicts.

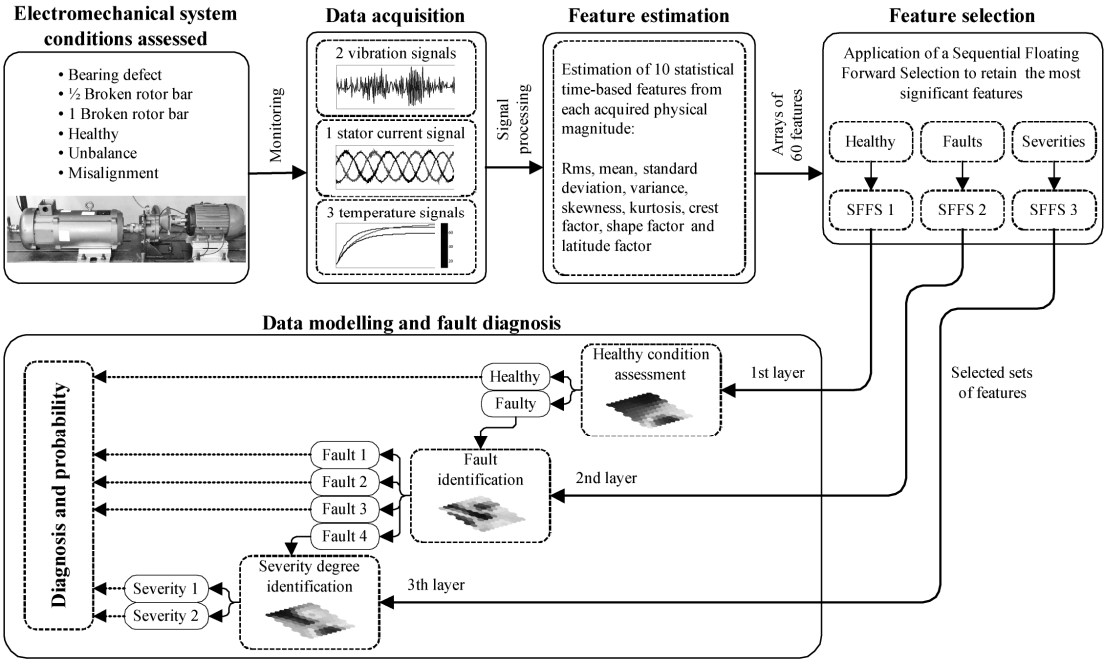

Fig. 2. Proposed diagnosis methodology based on a hierarchical SOM structure for identifying multiple faults in an induction motor.

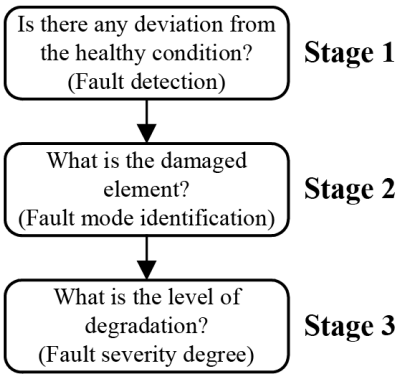

Fig. 3. General flowchart for the condition assessment of the electromechanical system.

As it was mentioned, the quantization error represents the distance from the input data vector, that is, the measurement under assessment, to its corresponding BMU during the SOM models evaluations. This information is proposed to be considered as a measure of the amount of previous knowledge that the SOM models have over such measurement, that is, a similarity degree in regard with the original data used during the training stage. Thus, in order to infer the reliability degree of the diagnosis outcome after each SOM evaluation, this information is proposed to be used. Indeed, during the training stage, the mapping of the input data vectors over their best matching units provides a mean quantization error, $\bar{E}_q$, that describes the average distance error between them. Thus, during the assessment of a new measurement, the resulting quantization error, E_q is analysed. Then, a E_q equal or less than the mean quantization error resulting from the SOM training process, $\bar{E}_q$, is associated with the highest reliability degree, $R = 1$, whereas an E_q bigger than the distance between the two further MUs, d_{max}, represents the lowest reliability degree $R = 0$. Finally, a E_q bigger than $\bar{E}_q$, and lower than d_{max}, will result in a reliability degree in the range between 1 and 0. Then, based in equation (2) the quantization error can be used to provide information related to the reliability of the condition monitoring.

$$R = \begin{cases} E_q \leq \overline{E_q}, & 1 \\ d_{max} > E_q > \overline{E_q}, & \frac{E_q - \bar{E}_q}{dmax - \bar{E}_q} - 1 \\ E_q > d_{max}, & 0 \end{cases} \quad (2)$$

4 EXPERIMENTAL SETUP

The experimental test bench used to validate the proposed multiple-fault diagnosis methodology is based on a kinematic chain composed by an IM, a gearbox and a DC generator. A flow chart of the experimental test bench is shown in Fig. 4(a). Specifically, the IM is a 1492-W three-phase IM, model WEG00236ET3E145T-W22, and to feed and control its rotational speed a variable frequency driver (VFD) is used, model WEGCFW08. Then, the IM is coupled to a 4:1 ratio gearbox, model BALDOR GCF4X01AA, driving its input shaft; subsequently, in turn, the output shaft of the gearbox drives the DC generator, model BALDOR-CDP3604, which is used as a mechanical load. A picture of the experimental test bench is shown in Fig. 3(b).

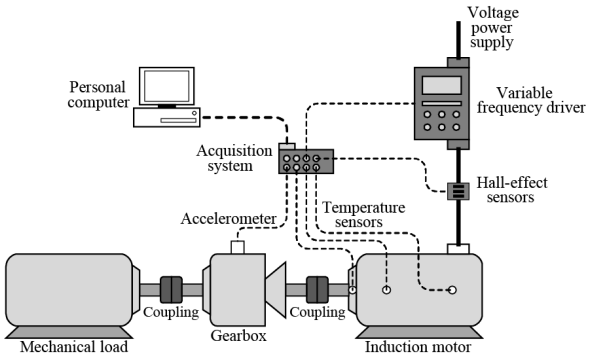

(a)

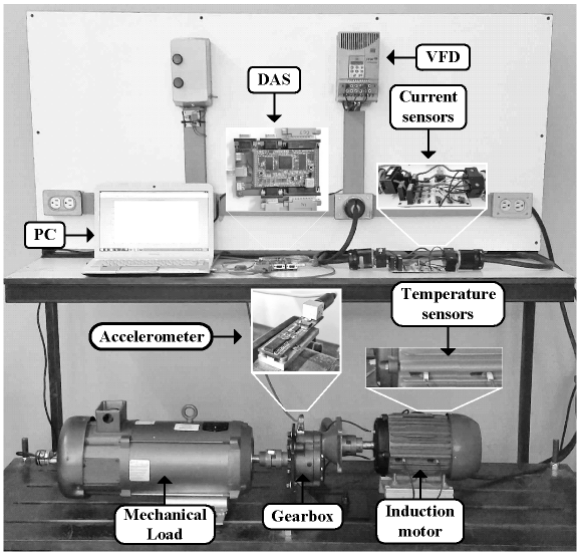

(b)

Fig. 4. Experimental test bench based on a kinematic chain used to validate the proposed diagnosis methodology. (a) Flow chart, wiring and mechanical connections. (b) Physical kinematic chain.

In this work, a set of different physical magnitudes are proposed to be acquired; in this regard, a tri-axial

accelerometer, model LIS3L02AS4, is fixed on the top of the gearbox to measure the vibration signatures. Although a tri-axial accelerometer has been used, only the perpendicular plane of the rotatory axis has been analyzed, since most of classical faults tend to affect the vibration modes in such axes. Moreover, it should be mentioned that the accelerometer is installed on the top of the gearbox due to it has been assumed that the occurrence of vibrations produced in the IM will travel through the kinematic chain; and consequently, are acquired by such sensor. On the other hand, in an industrial environment, the condition assessment may be performed by placing the vibration sensor in different parts of the machine. This assumption is asserted only if the vibration signals are acquired from the same. In this regard, the consideration of other different physical magnitudes may face and compensate the loss of information that is not acquired for the installed accelerometer sensor. Therefore, an IM stator current phase is acquired using a Hall-effect current sensor, model L08P050D15, from Tamura Corporation. In this proposal, just one stator current has been considered, however, if current phase imbalances are expected, the use of the three stator currents would be recommended. Besides, the temperature of the IM is also measured by means of three RTDs, model DM-301 from Labfancility LTD. One of the RTDs is placed at the bearing area in the frontal side of the IM, the other two RTDs are close to the rotor, in the lateral side of the IM. The installed accelerometers, Hall-effect sensor and RTDs, are mounted individually with its corresponding signal conditioning stage and its corresponding anti-alias filtering. To perform the data acquisition two 12-bit 4-channel serial-output sampling analog-to-digital converters, model ADS7841, from Texas Instruments are used as data acquisition system (DAS). The DAS is a development based on field programmable gate array technology which is a proprietary low-cost design. In order to perform a proper data acquisition, an analysis of the fault-frequency components that may be produced by the assessed electromechanical system was carried out. Thus, the sampling frequencies considered during the acquisition of vibrations, stator currents and temperatures are set to 3 kHz, 4 kHz and 1 kHz, respectively, and the DAS is programed for acquiring 300 kS, 400 kS and 100 kS, respectively, during 100 seconds when the IM is working during a steady-state regime. Indeed, it must be noted that previous to the data acquisition, the IM was started up to reach its thermal stability aiming that the temperature measurements were potentially significant to represent each one of the evaluated conditions. Besides, by considering different temperature signals is increased the potentiality of any fault detection and identification procedure, mainly, if these signals are acquired during the period of thermal stability of the IM and related components. Thus, the installation of temperature sensors in different places of the IM will provide meaningful information in regard with possible thermal patterns that may result from different fault conditions affectations. The consideration of different sampling frequencies plays an important role to perform the data acquisition during the condition monitoring; this is due to the different considered faults will tend to produce not similar effects over each one of the available physical magnitudes. That is, temperature is a physical magnitude of slow inertial, while vibration and stator current tend to respond in a faster way. Although different sampling frequencies are considered, it should be mentioned that the acquisition of vibrations and stator currents at the chosen frequencies will be enough if the frequency components and its harmonics related to considered faults would like to be analyzed. Besides, it should be mentioned that the acquired temperature signals are then subjected to digital decimation procedure and its frequency was reduced to 100 Hz.

Five different experimental conditions have been considered: healthy (HE), bearing defect (BD), broken rotor bar (BRB), unbalance (UNB) and misalignment (MAL). The IM uses a bearing model 6205-2ZNR, thus, a similar bearing has been damaged by means of drilling a through-hole on its outer race with a tungsten drill bit of 1.191 mm diameter to generate the BD. Two severity degrees of BRB fault are produced by drilling a hole of 6 mm diameter in two rotor bar elements: at depth of 3 mm, corresponding to 22% of the transversal section of the rotor bar, ½ BRB, and at depth of 14 mm, corresponding to a complete transversal section of the rotor bar, 1 BRB. The UNB condition has been induced by a bolt attachment to one of the IM couplings in order to produce a non-uniform load distribution that takes the center of mass out of the IM shaft. The MAL condition is generated moving 5 mm the free end of the IM on its horizontal plane, as a result, an angular misalignment of 1.5 degrees between shafts was approximately produced. This degree of misalignment is within the standards

that have been normally studied [8]. In Fig. 5 the set of faults artificially produced are shown. During the experimentation the IM is driven at different operating frequencies, that is, 5 Hz, 15 Hz and 50 Hz, producing an averaged rotating speed of 294 rpm, 890 rpm and 2985 rpm, respectively. Although the considered IM nominal frequency corresponds to 50 Hz, the use of lower operating frequencies, 5 Hz and 15 Hz, have been considered in order to make difficult the fault detection and identification due to the low speed levels produced. Thus, eighteen experiments, combining five different conditions and three operating frequencies, are considered. For each experiment, 100 one-second samples including information of all six acquired channels are available, thus, the available signals are segmented in equal part of one second to create a consecutive data set of samples.

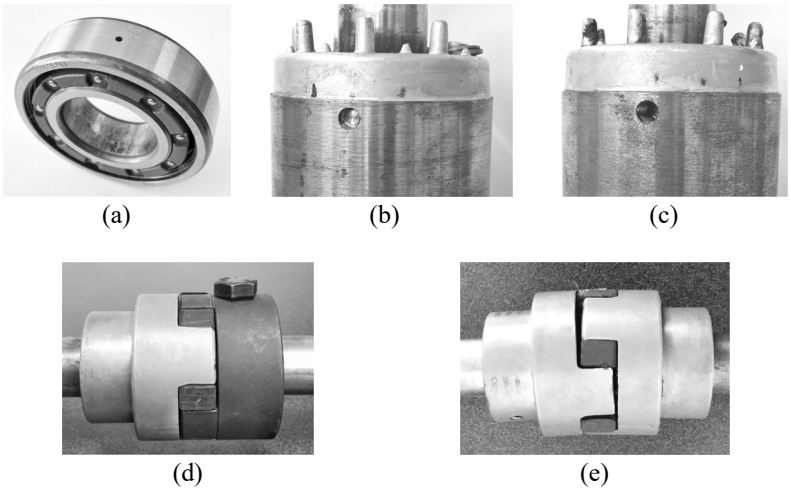

Fig. 5. Set of considered faults tested in the experimental test bench. (a) Bearing defect. (b) ½ Broken rotor bar. (c) 1 Broken rotor bar. (d) Unbalance. (e) Misalignment.

5 COMPETENCY OF THE METHOD

Previous to the analysis of the proposed condition monitoring scheme, a fault assessment through a classic characteristic fault frequencies analysis is performed in order to emphasize the current limitations in front of a multiple-fault scenario. Indeed, although the appearance of faults in electric machines can be detected through classical approaches by the estimation of specific characteristic fault features (i.e. Fourier transform following classical motor current signature analysis), the identification of such faults represents a major issue when multiple fault sources are considered simultaneously. In this sense, and considering the faults included in this work, the UNB and MAL conditions are fault scenarios that may generate similar effects over classical physical magnitudes acquired during the condition monitoring of a rotating electrical machine as vibration or stator current. That is, the UNB condition generates a centrifugal force leading to high vibration amplitudes frequencies equal to 1 x RPM (1 x rotational speed), in the spectral analysis; while the MAL condition results in high radial and/or axial vibration which typically produce dominant frequencies at 1 x RPM and/or 2 x RPM, depending upon the degree of angular misalignment against the offset misalignment [20]. Both fault conditions, UNB and MAL, also generate effects over the stator current spectrum that can be identified by specific characteristic fault-related frequencies. However, both conditions tend to produce similar stator current harmonics as follows; for the UNB condition the classical characteristic fault frequencies are described by (3).

$$f_{ecc} = f_s \left[1 \pm k\left(\frac{1-s}{p}\right)\right] = f_s \pm k f_r, \quad k = 1,2,\ldots \tag{3}$$

On the other hand, for the MAL condition, the characteristic fault frequencies occur through the appearance of sidebands around the fundamental current component [8], described by (4):

$$f_{sb} = f_s \pm k f_r, \quad k = 1,2,\ldots \tag{4}$$

where f_s is the electrical supply frequency, s is the unit-per slip, p is the number of pole pairs and f_r is the mechanical rotor peed.

Accordingly, by analyzing the theoretical effects that these faults may produce over the corresponding vibration and stator current signals, it can be concluded that both faults may appear overlapped, making more difficult the faults detection and their identification during the diagnosis assessment procedure and then, reducing the reliability of the condition monitoring system. In order to experimentally show such overlapping effect dealing with the MAL and UNB conditions, the vibration and the stator current signals in regard with the experimental test bench are analyzed. Thus, in Fig. 6 is shown the stator current spectrum at the closest region corresponding to $f_s + f_r$ when the supply frequency was set to 50Hz. From Fig. 6, it is possible to notice that the $f_s + f_r$ components of the UNB and MAL conditions appear at the same place. Although the amplitude of these components is slightly different, there is no practical difference to identify the actual machine condition since the amplitudes may be modified due to the fault severity; in this regard, the false negative detection ratios may be increased affecting the fault identification performance. Additionally, analysis performed through techniques based on frequency or time-frequency domains involve specific knowledge about the considered components under inspection and fault modes, such as information about electrical or mechanical characteristics and also the measurement of the rotational speed.

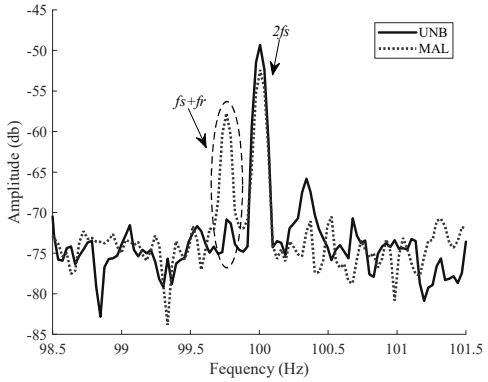

Fig. 6. Classic condition monitoring assessment based on the stator current spectrum at the closest region to f_s+f_r when the supply frequency is set to 50Hz.

Regarding the proposed condition monitoring method, in order to allow the hierarchical structure of the proposed multiple-fault detection and identification scheme the available data is grouped in different sets. Thus, in a first layer, the healthy or faulty condition of the kinematic chain is determined. In case of a fault diagnosis outcome, in a second layer the identification of the fault is carried out. Finally, in the third layer, the severity degree is determined, if available. Thereby, three data sets are designed. The first data set is formed by six-hundred samples defined by 60 statistical features each. In this first data set, there are 100 samples of the healthy condition per each of the three operating frequencies, that is, three hundred samples labeled as healthy (HLT). Also, 25 samples per each of the three operating frequencies and each of the four faults considered, that is, three hundred samples labeled as faulty (FLT). The second data set is formed by three-hundred samples defined by 60 statistical features each. In this second data set, there are 25 samples of the bearing defect condition per each of the operating frequencies, that is, seventy-five samples labeled as bearing defect (BD). There are 25 samples of the broken rotor bar condition per each of the operating frequencies, that is, seventy-five samples labeled as broken rotor bar (BRB). There are also 25 samples of the unbalance condition per each of the operating frequencies, that is, seventy-five samples labeled as unbalance (UNB). And also, there are 25 samples of the misalignment condition per each of the operating frequencies, that is, seventy-five samples labeled as misalignment (MAL). The third and last data set is formed by one-hundred and fifty samples defined by 60 statistical features each. In this third data set, there are 25 samples of half-broken rotor bar condition per each of the operating frequencies, that is, seventy-five samples labeled as half-broken rotor bar (1/2 BRB). Also,

there is 25 samples of one-broken rotor bar condition per each of the operating frequencies, that is, seventy-five samples labeled as one-broken rotor bar (1 BRB). In order to provide a detailed explanation in regard to the dataset generation, in Table 1 are summarized the datasets that will be evaluated in each one of the different layers that compose the proposed diagnosis method. Thus, each one of the datasets shown in Table 1 include detail information about labels of the different classes and number of samples. Yet, although 100 one-second samples are available for each considered condition, only the necessary samples of one second were used to create the described data sets.

First layer			Second layer			Third layer		
Label	Samples per condition	Total	Label	Samples per condition	Total	Label	Samples per condition	Total
HLT	(HLT)(100)(3)	300	BD	(BD)(25)(3)	75	½ BRB	(½ BRB)(25)(3)	75
FLT	(BD)(25)(3)	75	BRB	(BRB)(25)(3)	75	1 BRB	(1 BRB)(25)(3)	75
FLT	(BRB)(25)(3)	75	UNB	(UNB)(25)(3)	75			
FLT	(UNB)(25)(3)	75	MAL	(MAL)(25)(3)	75			
FLT	(MAL)(25)(3)	75						
		600			300			150

Table 1 - Resulting data sets generated to evaluate the proposed diagnosis methodology.

Once the three data sets are generated, the proposed feature selection procedure is applied individually to each of them in order to detect and remove the less significant features from the initial feature set. For each of the three dimensionality reduction procedures, the SFFS aims to optimize a model composed by a subset of the original feature set that best fits and describes the corresponding labels. In Table 2, the resulting selected features for each of the three data sets are shown. Thus, for the first layer to distinguish between healthy or faulty conditions, the selected subset of features results in eight statistical time features. In the second layer, where the fault condition is identified, the data set is reduced to sixteen statistical time features. In the third layer to determine the severity degree, the resulting set is composed by seven statistical time features. As the results show, the number of selected features change for each one of the layers; this variation is mainly related to the complexity of the problem that is solved. Specifically, the reduced number of eight selected features for the first layer, is due to the addressed problem is considered as a two-class problem. Then, the complexity of the problem increases in the second layer and the number of selected features increases to sixteen features because the number of classes that must be separated and classified also increases. Finally, for the third layer a reduced number of seven features is also selected due to only two severity conditions must be separated. It should be noted that, analyzing the results, statistical time features from different physical magnitudes are present in all set, thus, leading to an effective feature-level fusion approach. A qualitative representation of the resulting data manifolds of the first, second and third layer is shown in Fig. 7(a), Fig. 7(b) and Fig. 7(c), respectively, by means of a principal component analysis projection. In this regard, the three principal components considered in each projection exhibits an accumulative variance of 59.17%, for the first layer, 59.14% for the second layer, and 69.46% for the data third layer, which confirm the qualitative meaning of the representations. However, despite such qualitative sense, different clusters can be observed in the data distributions, which correspond to the affectation of the operating frequency conditions over the operating scenarios considered.

Physical magnitude	First layer	Second layer	Third layer
Vibration, tangential axis	$\bar{x}$	SF_{RMS}, CF and Ku	-
Vibration, radial axis	σ^2 and S_k	CF, IF and S_k	SF_{RMS}
Stator current	RMS	$\bar{x}$, SF_{RMS} and Ku	$\bar{x}$ and σ
Temperature 1	-	σ, SF_{RMS}, S_k and Ku	-
Temperature 2	$\bar{x}$ and S_k	$\bar{x}$ and σ	RMS, σ^2, SF_{RMS} and Ku
Temperature 3	LF and S_k	S_k	-

1 **Table 2 - Resulting subsets of selected features by means of SFFS.**
2

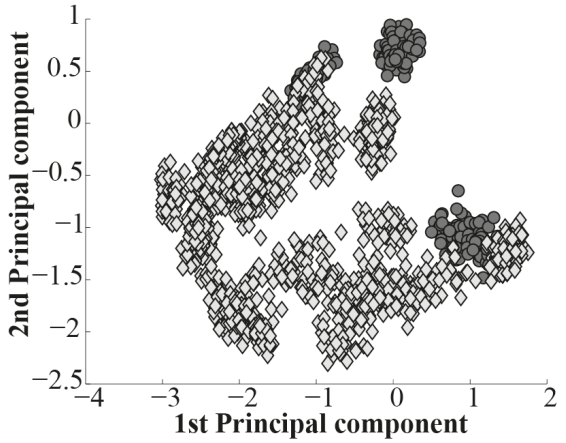

(a)

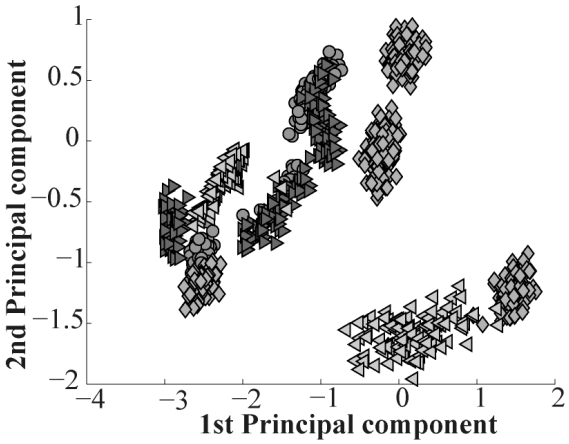

(b)

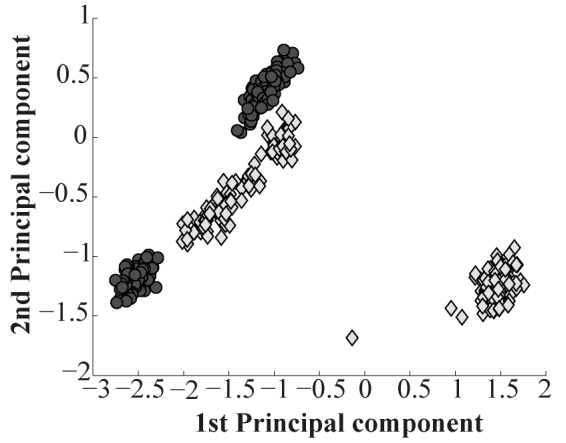

(c)

Fig. 7. PCA projections over the resulting selected sets of features for each of the three layers. (a) First layer's data, HLT condition, ●, and FLT condition, ◇. (b) Second layer's data, BD condition, ○, BRB condition, ◇, UNB condition, ▶, and MAL condition, ◁. (c) Third layer's data, ½BRB condition, ●, and 1BRB condition, ◇.

1

Next, the modelling of such data set manifolds described by the selected sets of features is carried out by means of SOM. In this sense, the U-matrix represents the resulting mapping for each one of the considered SOM, in which the distances among neurons are represented. According to the proposed diagnosis scheme, and following the previous dimensionality reduction stage, three SOM instances are carried out. The first SOM, SOM_1, is considered to model and determine later, the healthy or faulty condition of the kinematic chain, Fig. 8(a). The second SOM, SOM_2, is considered to model and determine later, the fault condition of the kinematic chain, Fig. 8(b). Finally, the third SOM, SOM_3, is considered to model and determine later, the fault severity degree, Fig. 8(c).

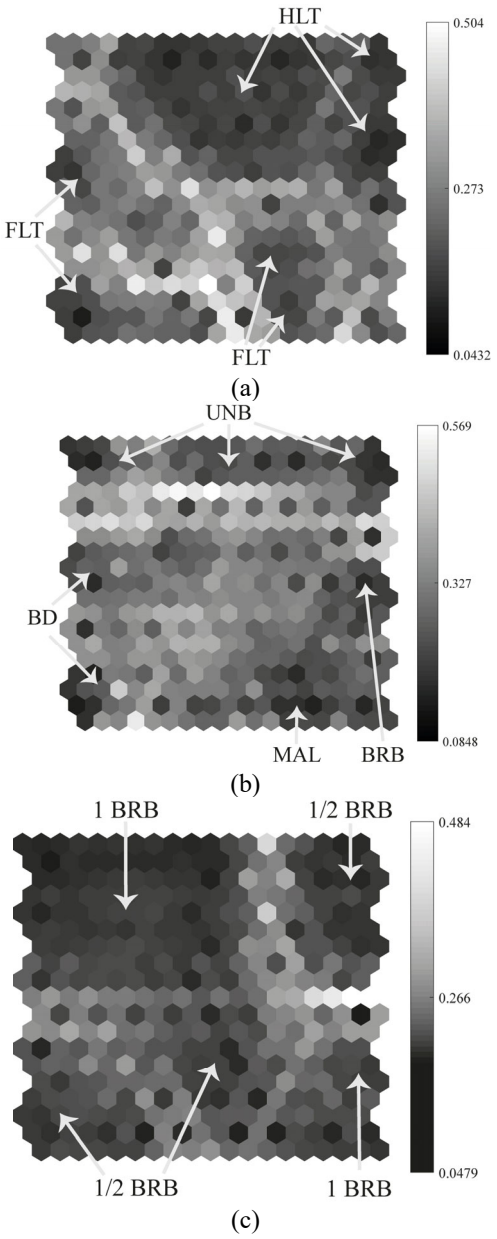

Fig. 8. SOM's U-matrixes over the resulting selected sets of features for each of the three layers. The lighter the color between two neuron units in the U-matrix is, the larger is the relative distance between them. (a) SOM_1 U-matrix, first layer's data, HLT and FLT conditions. (b) SOM_2 U-matrix,

The three SOM instances have been initialized as 2-dimensional hexagonal grids of 10 x 10 neurons, that represents a total of 100 neurons to model the data manifolds during a 100 epochs batch algorithm training. It can be seen that each of the resulting SOM reveals different number and distribution of data clusters similarly to the PCA projections, represented by sets of near neurons far from other neuron groups. Thus, from the U-matrix of SOM_1, Fig. 8(a), it is appreciated a main data cluster, corresponding to the healthy condition, and other smaller clusters belonging to the rests of faulty evaluated conditions. Also, in Fig. 8(b), from the resulting U-matrix of SOM_2, shows a set of clusters, corresponding to the different faulty conditions considered. Finally, from the U-matrix of SOM_3 depicted in Fig. 8(c), different data clusters related to the two different severities of BRB fault condition are revealed. From the SOM training procedures, Q_{error} mean values of 0.21, 0.39 and 0.13 are obtained for SOM_1, SOM_2 and SOM_3, respectively. Also, a Q_{error} kurtosis values of 3.84, 3.96 and 3.73, is obtained for SOM_1, SOM_2 and SOM_3, respectively, which means that measurements are normally distributed.

Indeed, during the SOM training procedure, each initial neuron grid is adapted to the data manifold in order to preserve as much as possible the topological characteristics of the corresponding distribution. The SOM application is an unsupervised technique by nature, however, as it has been explained, the assignment of corresponding labels for each neuron after the corresponding SOM training is proposed. That is, each of the SOM neurons adopts, by a majority voting approach of the nearest data samples, the resulting label. In this regard it can be seen, in Fig. 9(a), that the resulting SOM_1 is divided in two regions, the HLT condition and the FLT condition. In Fig. 9(b) four different classes are represented, BD, BRB, UNB and MAL. In Fig. 9(c) the two severities of broken rotor bar, that is, the ½BRB and the 1BRB, are represented.

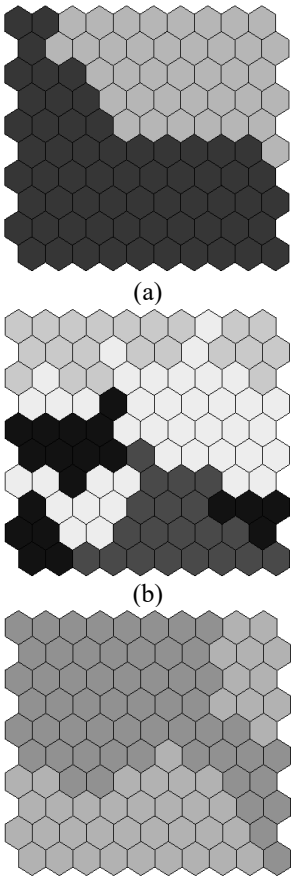

Fig. 9. Resulting SOM classification maps. (a) *SOM1*, HLT condition, ⬡, and FLT condition, ⬢.(b) *SOM2*, BD condition, ⬢, BRB condition, ⬡, UNB condition, ⬡, and MAL condition, ⬢.(c) *SOM3*, ½BRB condition, ⬡, and 1BRB condition, ⬢.

Then, a new measurement, once characterized by the corresponding set of features, is evaluated sequentially over the diagnosis layers following the proposed hierarchical evaluation rules. Thus, during each layer assessment, the label of the corresponding BMU is obtained. Also, the corresponding reliability value is estimated by combining partial reliability assessments following (2) and (5). It must be noted that in case of just one or two layer assessment, the reliability associated to the rest of not-evaluated layers is considered as 1.

$$R_{Total} = R_{SOM_1} * R_{SOM_2} * R_{SOM_3} \quad (5)$$

Thus, each SOM model, preceded by its SFFS, represents a diagnosis layer, and the three diagnosis layers together comprise the proposed diagnosis structure that allows to obtain a diagnosis outcome with its corresponding reliability value.

In this regard, considering the data subsets presented in Table 1, for each dataset that corresponds to the evaluated layer, four-fifth of the data has been used for training and one-fifth for test purposes during each of the 5-fold iterations. That is, i.e. for the first layer, 240 samples of the HLT condition are used for training purposed and 60 samples for the evaluation. Additionally, 60 samples from each faulty condition (240 samples considering all conditions) are used also during the training and 15 samples from each faulty condition are used for the evaluation (60 samples in total for considering all condition). Thereby, in Table 3 the aggregated confusion matrix computed during the training and test of the *SOM1* is shown. The corresponding classification ratio achieved is 99.8% and 100% for the training and test, respectively. Similarly, in Table 4, the aggregated confusion matrix computed during the training and test of the *SOM2* is shown. The corresponding classification

ratio achieved is 94.2% and 92.5% for the training and test, respectively. Finally, in Table 5, the aggregated confusion matrix computed during the training and test of the SOM_3 is shown. The corresponding classification ratio achieved is 98.3 % and 99.2 % for the training and test, respectively. It must be noticed that for all diagnosis outcomes, the corresponding reliability ratio was above 90%.

		Training		Test	
		Actual			
Estimation		HLT	FLT	HLT	FLT
	HLT	240	1	60	0
	FLT	0	239	0	60

Table 3 – Confusion matrix of first layer, SOM_1.

		Training				Test			
		Actual							
		BD	BRB	UNB	MAL	BD	BRB	UNB	MAL
Estimation	BD	222	4	0	10	58	0	0	8
	BRB	7	219	5	2	1	54	2	0
	UNB	0	10	235	0	0	5	58	0
	MAL	11	7	0	228	1	1	0	52

Table 4 - Confusion matrix of second layer, SOM_2.

		Training		Test	
		Actual			
Estimation		½ BRB	1 BRB	½ BRB	1 BRB
	½ BRB	237	3	60	1
	1 BRB	3	237	0	59

Table 5 - Confusion matrix of third layer, SOM_3.

In order to highlight the complexity of the considered data set and the superiority of the proposed multiple-fault detection and identification scheme, a comparison of the obtained results against those that may be obtained by classical approaches is performed. In this regard, classical data-driven approaches have been implemented considering the two most used variants for dimensionality reduction, that is, PCA and LDA, in combination with NN for pattern recognition. The PCA has been configured to retain more than 90% of variance from the original 60-dimensional input space. Also, the LDA has been configured retaining all features from the 80-*th* percentile in terms of maximum individual Fischer score revealed. The NN has been structured with one hidden layer composed by double number of neurons than the corresponding input layer. The analysis has been extended to the use of just one physical magnitude, that is, initial statistical time features from vibration, stator current or temperature, as well as the use of the whole feature sets of all signals. In Table 6 the resulting classification accuracies of such eight variants are summarized. This results clearly shown a lower performance of the diagnosis results for all variants in the classical framework. Most of electromechanical multi-fault problems exhibit a non-Riemannian data manifold in the considered feature space, that is, the feature vectors used to characterize the measurements behave as a disconnected sub-manifolds or clusters. Indeed, PCA seeks for a global structure of the data and, then, false data distribution characteristics are considered. On the other hand, although the LDA optimization function deals with multiple-class separation problems, the complexity of a whole multi-fault diagnosis scenario leads to global projections of the data, where specific classes separation opportunities are discarded for the sake of the global Fischer parameter estimation. Moreover, in regard with results of Table 6 performed by classic approaches, the classification performance is significantly improved by means of applying the proposed hierarchical structure. Indeed, from a collaborative point of view, due to the proposed method has the capability of filter automatically those features revealing hidden significant

information, the consideration of a statistical time-domain set features extracted from vibration, stator currents and temperatures increase the identification of malfunctioning conditions. Thereby, the increase of performance resulting from the proposed multiple-fault identification scheme is, in part, due, to the hierarchical organization, since multiple operating frequencies and conditions considered lead to an increase of discrimination complexity. Furthermore, the proposed method also has the advantage of be highly adaptive to any domain of processing signals and estimated set of features. For this reason, the hierarchical structure proposes gathering similar data under a same label, and identifies gradually the patterns by a non-linear and performative approach resulting from the SFFS and SOM combination.

Physical magnitude/s considered	PCA+NN		LDA+NN	
	Training	Test	Training	Test
Vibrations	45.5 %	39.2 %	59.4 %	56.4 %
Stator current	40.5 %	34.2 %	62.1 %	55.0 %
Temperatures	65.3 %	60.0 %	67.6 %	56.7 %
All	64.4 %	62.2 %	61.3 %	63.1 %

Table 6 – Resulting classification ratios obtained with classical diagnosis approaches by means of LDA or PCA, and NN, with different physical magnitude sets.

6 CONCLUSIONS

This work presents a novel diagnosis methodology for detection and identification of multiple faults in a kinematic chain driven by an induction motor under different operating frequencies. There exist third important aspects that should be highlighted about the proposed method. First, it is demonstrated that the use of different physical magnitudes allows to reach a better characterization of the different conditions assessed. Indeed, each one of the considered physical magnitudes reveals different capabilities to reflect the evaluated fault conditions; even more, by performing a feature-level fusion of these physical magnitudes through a statistical time-based characteristic, a high-performative high-dimensional feature set is built. Second, the application of an initial soft-feature selection stage based on SFFS over the original data sets allows to remove those features with the less discriminative capabilities, and the significance of the resulting sets for each of the considered layers is improved. Third, the consideration of a hierarchical structure based on SOM represents a high-performing approach dealing with a multiple-fault detection and identification, since the measurement under analysis is assessed gradually over modelled data manifolds that maintain the underlying physical phenomena taking place at the system under monitoring. In this work, six different conditions evaluated at three different operating frequencies have been assessed. It must be emphasized that under all these conditions, the proposed multiple-fault detection and identification scheme exhibits a classification ratio of 91.57%. In comparison with classical diagnosis structures, the proposed methods improve the global classification ration by a 30% approximately. The obtained results make the proposed diagnosis methodology suitable to be applied for assessing the condition of kinematic chain driven by induction motor, and represents a promising diagnosis scheme to be applied to other faults and electric motor technologies in industrial applications.

ACKNOWLEDGEMENTS

This research work has been partially supported by CONACYT, Mexico, under doctoral scholarship number 278033 and by the Spanish Ministry of Economy and Competitiveness under the TRA2016-80472-R.

REFERENCES

[1] M. Riera-Guasp, J. A. Antonino-Daviu and G. A. Capolino, “Advances in electrical machine, power electronic, and drive condition monitoring and fault detection: State of the art,” *IEEE Transactions on Industrial Electronics*, vol. 62, no. 3, pp. 1746-1759, March 2015.

[2] T. Ince, S. Kiranyaz, L. Eren, M. Askar and M. Gabbouj, “Real-time motor fault detection by 1-D convolutional neural networks,” *IEEE Transactions on Industrial Electronics*, vol. 63, no. 11, pp. 7067-7075, Nov. 2016.

[3] M. Tsypkin, “The origin of the electromagnetic vibration of induction motors operating in modern industry: Practical experience, analysis and diagnostics,” *IEEE Transactions on Industry Applications*, vol. 53, no. 2, pp. 1669-1676, March-April 2017.

[4] N. R. Devi, D. V. S. S. S. Sarma and P. V. R. Rao, "Detection of stator incipient faults and identification of faulty phase in three-phase induction motor – simulation and experimental verification," *IET Electric Power Appl.*, vol. 9, Issue. 8, pp. 540-548, 2015.

[5] R. H. Cunha Palacios, I. N. da Silva, A. Goedtel and W. F. Godoy, "A novel multi-agent approach to identify faults in line connected three-phase induction motors," *Applied Soft Computing*, vol. 45, pp. 1-10, 2016.

[6] S. B. Lee, D. Hyun, T. J. Kang, C. Yang, S. Shin, H. Kim, S. Park, T. S. Kong and H. D. Kim, "Identification of false rotor fault indications produced by online MCSA for medium-voltage induction machines," *IEEE Trans. Ind. Appl.*, vol. 52, no. 1, pp 729-739, 2016.

[7] L. Saidi, J. B. Ali, F. Fnaiech, "Application of higher order spectral features and support vector machines for bearing faults classification," *ISA Transactions*, vol. 54, pp. 193-206, 2015.

[8] C. Verucchi, J. Bossio, G. Bossio and G. Acosta, "Misalignment detection in induction motors with flexible coupling by means of estimated torque analysis and MCSA," *Mech. Syst. Signal Process.*, vol. 80, pp. 570-581, 2016.

[9] P. Gansgar and R. Tiwari, "Comparative investigation of vibration and current monitoring for prediction of mechanical and electrical faults in induction motor based on multiclass-support vector machine algorithms," *Mech. Syst. Signal Process.*, vol. 94, pp. 464-481, 2017.

[10] R. K. Patel and V. K. Giri, "Analysis and interpretation of bearing vibration data using principal component analysis and self-organizing map," *Inter. J. Advanced Design and Manufacturing Technology*, vol. 9, no.1, pp. 111-117, 2016.

[11] A. Glowacz and Z. Glowacz, "Diagnosis of three-phase induction motor using thermal imaging," *Infrared Physics & Technology*, vol. 81, pp. 7-16, 2017.

[12] L. Jing, T. Wang, M. Zhao and P. Wang, "An adaptive multi-sensor data fusion method based on deep convolutional neural networks for fault diagnosis of planetary gearbox," *Sensors*, vol. 17, Issue 2, pp. 1-15, 2017.

[13] M. Tsypkin, "The origin of vibration of induction motors operating in modern industry: Practical experience – Analysis and Diagnostics," *IEEE Trans. Ind. Appl.*, vol. 53, no. 2, pp. 1760-1769, 2017.

[14] S. Haroun, A. N. Seghir and S. Touati, "Feature selection for enhancement of bearing fault detection and diagnosis based on self-organizing map," *Recent Advances in Electrical Engineering and Control Applications*, vol. 411, pp. 233-246, 2017.

[15] P. Baraldi, F. Cannarile, F. Di Maio and E. Zio, "Hierarchical k-nearest neighbors classification and binary differential evolution for fault diagnostics of automotive bearings operating under variable conditions," *Engineering Appl. of Artificial Intelligence*, vol. 56, pp. 1-13, 2016.

[16] J. J. Saucedo, M. Delgado-Prieto, J. A. Ortega, R. A. Osornio-Rios and R. J. Romero-Troncoso, "Multiple-Fault Detection Methodology Based on Vibration and Current Analysis Applied to Bearings in Induction Motors and Gearboxes on the Kinematic Chain," *Shock and Vibration*, vol. 2016, pp. 1-13, 2016.

[17] V. H. Jaramillo, J. R. Ottewill, R. Dudek, D. Lepiarczyk and P. Pawlik, "Condition monitoring of distributed systems using two-stage Bayesian inference data fusion," *J. Mech. Syst. Signal Process.*, vol. 87, Part A, pp 91-110, 2016.

[18] J. J. Saucedo-Dorantes, M. Delgado-Prieto, R. A. Osornio-Rios and R. J. Romero-Troncoso, "Diagnosis methodology based on statistical-time features and linear discriminant analysis applied to induction motors," *in Proceedings of the IEEE 11th International Symposium on Diagnostics for Electrical Machines, Power Electronics and Drives.*, pp. 517-523, IEEE, Tinos, Greece, August-September 2017.

[19] C. Wang, M. Gan and C. Zhu, "Fault feature extraction of rolling element bearings based on wavelet packet transform and sparse representation theory," *Journal of Intelligent Manufacturing*, vol. 1, pp 1-15, 2015.

[20] J. D. Martínez-Morales, E. R. Palacios-Hernández and D. U. Campos-Delgado, "`Multiple-fault diagnosis in induction motors through support vector machine classification at variable operating conditions", *Electrical Engineering*, vol. 100, pp. 59-73, 2018.

[21] A. Soualhi, G. Clerc and H. Razik, "Detection and diagnosis of faults in induction motor using an improved artificial ant clustering technique," *IEEE Transactions on Industrial Electronics*, vol. 60, no. 9, pp. 4053-4062, 2013.

[22] S. Yu, J. Qing-Chao and Y. Xue-Feng, "Fault diagnosis and process monitoring using a statistical pattern framework based on a self-organizing map," *J. Central South University*, vol. 2, no. 2, pp. 601-609, 2015.

[23] M. Kam, J. Kim, J. M. Kim, A. C. C. Tan, E. Y. Kim and B. C. Choi, "Reliable fault diagnosis for low-speed bearings using individually trained support vector machines with kernel discriminative feature analysis,"*IEEE Trans. Power Electron.*,vol.30,no.5,pp.2786-2797, 2015.

[24] T. W. Rauber, F. A. Boldt and F. M. Varejao, "Heterogeneous feature models and feature selection applied to bearing fault diagnosis," IEEE Transactions on Industrial Electronics, vol. 62, no. 1, pp 637-646, 2015.

[25] A. Sharma and K. K. Paliwal, "Linear discriminant analysis for the small sample size problem: an overview," *Inter. J. Machine Learning and Cybernetics*, vol. 6, no. 3, pp 443-454, 2015.

[26] C. Jing and J. Hou, "SVM and PCA based fault classification approaches for complicated industrial process," *Neurocomputing*, vol. 167, pp. 636-642, 2015.

[27] J. Harmouche, C. Delpha and D. Diallo, "Improved fault diagnosis of ball bearings based on the global spectrum of vibration signals," *IEEE Trans. Energy*, vol. 30, no. 1, pp 376-383, 2015.

[28] M. Kang, J. Kim and J. M. Kim, "Reliable fault diagnosis for incipient low-speed bearings using fault feature analysis based on a binary bat algorithm," *Information Sciences*, vol. 294, pp 423-438, 2015.

[29] L. Lu, J. Yan and C. W. de Silva, "Dominant feature selection for the fault diagnosis of rotatory machines using modified genetic algorithm and empirical mode decomposition," *J. Sound and Vibration*, vol. 344, pp 464-483, 2015.

[30] O. Janssens, V. Slavkovikj, B. Vervisch, K Stockman, M. Loccufier, S. Verstockt, R. V. Walle and S. V. Hoecke, "Convolutional neural network based fault detection for rotating machinery," *J. Sound and Vibration*, vol. 377, pp.331-345, 2016.

[31] H. C. Chang, S. C. Lin, C. C. Kuo and C. F. Hsieh, "Induction motor diagnostic system based on electrical detection method and fuzzy algorithm," *Inter. J. Fuzzy Systems*, vol. 18, Issue 5, pp 732-740, 2016.

[32] W. Sun, S. Shao, R. Zhao, R. Yan, X. Zhang and X. Chen, "A sparse auto-encoder-based deep neural network approach for induction motor faults classification," *Measurement*, vol. 89, pp 171-178, 2016.

[33] S. M. Erfani, S. Rajasegarar, S. Karynasekera and C. Leckie, "High-dimensional and large-scale anomaly detection using a linear one-class SVM with deep learning," *Pattern Recogn.*, vol. 58, pp 121-134, 2016.

[34] S. Haroun, A. N. Seghir and S. Touati, "Feature selection for enhancement of bearing fault detection and diagnosis based on Self-Organizing Map," *Recent Advances in Electrical Engineering and Control Applications*, vol. 411, pp 233-246, 2017.

[35] J. Yu, "Local and Nonlocal Preserving Projection for Bearing Defect Classification and Performance Assessment," *IEEE Trans Ind. Electron.*, vol. 59, no. 5, pp. 2363-2376, May 2012.
[36] J. Tang and X. Yan, "Neural network modeling relationship between inputs and state mapping plane obtained by FDA-t-SNE for visual industrial process monitoring," *Applied Soft Computing*, vol. 60, pp. 557-590, 2017.
[37] A. A. Akinduko, E. M. Mirkes, A. N. Gorban, "SOM: Stochastic initialization versus principal components," *Information Sciences*, vol. 364-365, pp. 213-221, 2016.
[38] M. A. Valle, G. A. Ruz, V. H. Masías, "Using self-organizing maps to model turnover of sales agents in a call center," *Applied Soft Computing*, vol. 60, pp. 763-774, 2017.
[39] G. Singh, T.Ch. A. Kumar and V. N. A. Naikan, "Induction motor inter turn fault detection using infrared thermographic analysis," *Infrared Physics & Technology*, vol. 77, pp. 277-282, 2016.

Juan Jose Saucedo-Dorantes received the M. E. and Ph. D degrees in mechatronics from the Autonomous University of Queretaro (UAQ), Queretaro, Mexico, in 2014 and 2018, respectively. Since 2012, he has been doing research work at the HSPdigital group. He is currently working as a researcher at the Engineering Faculty, UAQ, Queretaro, Mexico. His research interest include digital signal processing on FPGAs for applications in engineering, condition monitoring and fault diagnosis in electromechanical systems, fault detection algorithms, artificial intelligence and signal processing methods.

Miguel Delgado-Prieto received the M.S. and Ph.D. degrees in Electronics Engineering from the Universitat Politècnica de Catalunya, UPC, Barcelona, Spain in 2007 and 2012, respectively. In 2008 he joined the MCIA Research Center of the Electronic Engineering Department of the UPC where, currently, he carries out research and technology transfer activities at national and international level. From 2004 he has occupied different teaching positions at the UPC, where he is currently adjunct lecturer in the Electronic Engineering Department. His research interests include fault diagnosis in electromechanical machines, fault-detection algorithms, machine learning, signal processing methods and digital systems.

Rene de J. Romero-Troncoso received the Ph.D. degree in mechatronics from the Autonomous University of Queretaro, Queretaro, Mexico, in 2004. He is a National Researcher level 3 with the Mexican Council of Science and Technology, CONACYT. He is currently a Head Professor with the University of Guanajuato and an Invited Researcher with the Autonomous University of Queretaro, Mexico. He has been an advisor for more than 200 theses, an author of two books on digital systems (in Spanish), and a coauthor of more than 130 technical papers published in international journals and conferences. His fields of interest include hardware signal processing and mechatronics. Dr. Romero–Troncoso was a recipient of the 2004 Asociación Mexicana de Directivos de la Investigación Aplicada y el Desarrollo Tecnológico Nacional Award on Innovation for his work in applied mechatronics, and the 2005 IEEE ReConFig Award for his work in digital systems. He is part of the editorial board of Hindawi's International Journal of Manufacturing Engineering.

Roque A. Osornio-Rios received the Ph.D. degree in mechatronics from the Autonomous University of Queretaro, Queretaro, Mexico, in 2007. Dr. Osornio-Rios is a National Researcher level 2 with the Mexican Council of Science and Technology, CONACYT. He is currently a Head Professor with the University of Queretaro, Mexico. He is advisor for more than 80 theses, and a coauthor of more than 90 technical papers published in international journals and conferences. His fields of interest include hardware signal processing and mechatronics. Dr. Osornio-Rios is fellow of the Mexican Academy of Engineering. He is part of the editorial board of Journal and Scientific and Industrial Research.